ACS OMEGA

http://pubs.acs.org/journal/acsodf

Article

Flexible Ternary Combination of Gellan Gum, Sodium Carboxymethyl Cellulose, and Silicon Dioxide Nanocomposites Fabricated by Quaternary Ammonium Silane: Rheological, Thermal, and Antimicrobial Properties

Balasubramanian Rukmanikrishnan, Chaehyun Jo, Seungjin Choi, Srinivasan Ramalingam, and Jaewoong Lee*

Cite This: *ACS Omega* 2020, 5, 28767−28775

Read Online

ACCESS | Metrics & More | Article Recommendations | Supporting Information

ABSTRACT: Gellan gum−sodium carboxymethyl cellulose (GC)-based composite films with various concentrations of silicon dioxide (SiO_2) nanoparticles and octadecyldimethyl-(3-triethoxy silylpropyl)ammonium chloride (ODDMAC) were successfully prepared by the traditional solution casting method to improve the antimicrobial and water repellent properties. Fourier transform infrared (FT-IR) spectra confirm the formation of hydrogen bonds between the GC and nano-SiO_2. The microstructure and physicochemical properties were investigated by FT-IR, wide-angle X-ray diffraction, and scanning electron microscopy (SEM) analyses. The rheological properties of the GC−SiO_2 hydrogel were also characterized. The results show that the inclusion of SiO_2 nanoparticles significantly improved the viscosity and viscoelastic properties of the GC hydrogel. The GC−SiO_2 hydrogel exhibited shear-thinning behavior and its viscosity decreased at high shear rates. The storage and loss moduli of the GC composites increased as the frequency and SiO_2 concentration increased. The tensile strength and elongation at break of the GC composites increased by 75.9 and 62%, respectively, with the addition of SiO_2 and ODDMAC. In addition, nano-SiO_2 decreased the water vapor permeability and increased the hydrophobic properties of the GC−SiO_2 composites. Thermogravimetric analysis showed that the $T_{5\%}$ loss was in the range of 99.4−128.6 °C and the char yield was in the range of 20.1−29.9%, which was significantly enhanced by the incorporation of SiO_2 nanoparticles. The GC−SiO_2 (ODDMAC) nanocomposites effectively shielded the UV light and exhibited high antimicrobial activity against six different pathogens. The simple and cost-effective GC−SiO_2 (ODDMAC) nanocomposites gained importance in food packaging and biomedical applications.

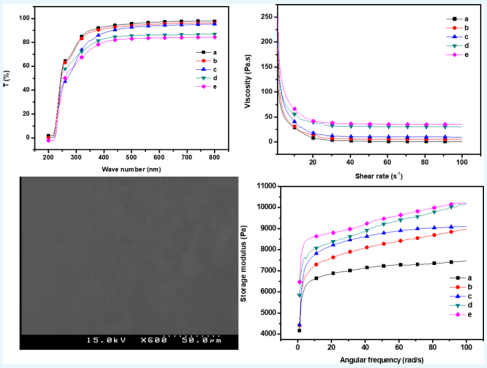

1. INTRODUCTION

Biopolymer-based sustainable composites have been developed over several decades and have recently gained much attention as viable alternatives to nonbiodegradable polymer composites due to their nontoxicity, biocompatibility, biodegradability, wide availability, and favorable cost.[1−3] However, their processing and physical properties are still insufficient for many applications. This can be attributed to a low molecular weight, low crystallinity, high moisture uptake, and poor mechanical properties. Cellulose is the most attractive polymer because of its strong inter and intramolecular hydrogen bonds, making it insoluble in water and most common organic solvents.[1,4,5] The modification of the cellulose structure generally enables its use in various applications, such as laminate coatings, optical films, food, and pharmaceuticals.

Cellulose is the most abundant renewable resource in nature. It is a nontoxic, biodegradable, and biocompatible material, which makes it an excellent choice for the preparation of composites with numerous potential applications.[6] Sodium carboxymethyl cellulose is the most compatible water-soluble polymer. It is mainly used in food additives as a smoothing agent, thickener, phase and emulsion stabilizer, and suspending agent, among other applications for many decades.[7−10]

Gellan gum is a bacterial polysaccharide consisting of tetrasaccharide-repeating units of D-glucose, D-glucuronic acid, and L-rhamnose. It has recently received attention in many tissue and biomedical applications owing to its biocompatibility and low cytotoxicity. Gellan gum can be conveniently processed into hydrogels that are resistant to heat and acid. However, its application is limited by its relatively high gelation temperature and insufficient mechanical strength. In addition,

Received: August 24, 2020
Accepted: October 14, 2020
Published: October 27, 2020

their properties can be improved by the addition of carboxymethyl cellulose-based materials.[1,11,12]

Two or more polymers can be used in the formulation of biopolymers to achieve a synergistic effect between the polymer properties. In general, the combination of biopolymers influences the rheological properties.[13] Therefore, the composites prepared with gellan gum and carboxymethyl cellulose may overcome the intrinsic limitations of gellan gum. Although blended biopolymer films are promising food packaging materials, their poor mechanical properties, high water sensitivity, and low resistance to moisture limit their applications.[14]

The addition of nanofillers, such as carbon nanotubes, graphene oxide, clay, zinc oxide, titanium dioxide, and silicon dioxide (SiO_2, silica), into blended biopolymer films has attracted much attention due to their outstanding potency, barrier, mechanical, optical, electrical, and flame-retardant properties.[6,15] Silica has been used as a new generation of nanomaterials to prepare polymer hybrids because it possesses the advantages of light mass, low cost, high abundance, high strength, high modulus, and high thermal stability.[14] Silica is natural, and it can be used to develop smart polymer–inorganic composite materials. It has a smooth, large surface area and nonporous surface, which could assist strong physical contact between the polymer and filler matrixes.[16,17] Rheological studies on biopolymer composite solutions can help us to understand the structural relationship between the polymer and nanoparticles and to optimize the production of nanostructured films, especially when using the casting and spreading techniques.[18−20]

The antimicrobial properties of food packaging materials have attracted important and considerable interest owing to their potential benefits. Quaternary ammonium silanes (QASs) containing long alkyl chain carbon atoms have been widely used against various microorganisms in different fields such as food, cosmetics, pharmaceuticals, disinfectants, and water treatment. This novel combination of quaternary ammonium silane and silica nanoparticles with the gellan gum–sodium carboxymethyl cellulose (GC) composite provided inspiration and broad prospects in the field of food packaging applications.[21−23] There has been no similar study to date examining in detail the properties of nanocomposites for food packaging applications. In this study, we aim at enhancing the thermal and mechanical strength of a gellan gum–sodium carboxymethyl cellulose–silica (GC–SiO_2) nanocomposite film. In addition, we study the antimicrobial effect of adding long alkyl chains containing silica nanoparticles to GC–SiO_2 nanocomposites.

2. RESULTS AND DISCUSSION

2.1. Fourier Transform Infrared (FT-IR) Analysis. The FT-IR spectra of the prepared nanocomposite films shown in Figure 1. The hydroxyl (OH) and C═O stretching peaks of the carboxylate group appeared at 3431 and 2820 cm^{-1}, respectively. The alkyl ester groups in the gellan gum exhibited characteristic bands at 1401 (C–H methyl groups) and 1719 (C═O) cm^{-1}. The glycosidic linkage in the gellan gum appeared at 1611 cm^{-1}. The broad peak at 3358 cm^{-1} in the composite film spectra is ascribed to the stretching vibrations of the OH and C–H groups, whereas the peaks at 1589 and 1321 cm^{-1} were assigned to the asymmetric (C═O) and symmetric (C–O) stretching vibrations, respectively. The bands at 1158, 1059, and 1030 cm^{-1} were due to the

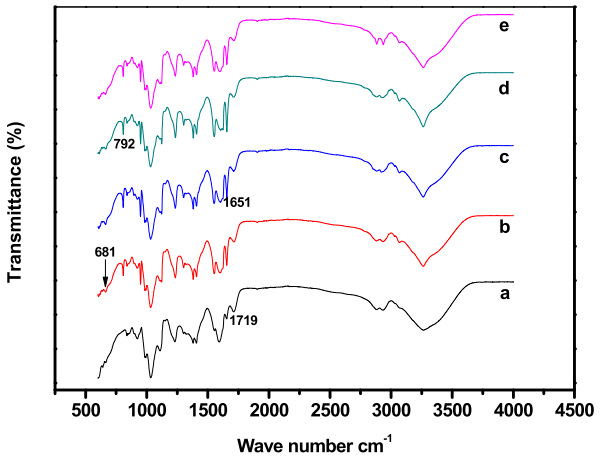

Figure 1. FT-IR spectra of (a) GC, (b) GC–SiO_2-1, (c) GC–SiO_2-3, (d) GC–SiO_2-5, and (e) GC–SiO_2-5 with ODDMAC.

symmetric stretching vibration of C–O–C and include the skeletal vibration of the C–O stretching.[1] The FT-IR spectra of the GC–SiO_2 composites exhibit –OH stretching peaks at 3384 and 1102 cm^{-1}, corresponding to the stretching vibration of Si–O–Si. The characteristic peak of the silica structure is usually found in the range of 1300–600 cm^{-1}. The peaks at 1081 and 790 cm^{-1} can be assigned to the asymmetric and symmetric vibrations of the siloxane linkages (Si–O–Si) in the SiO_4 tetrahedra, respectively. The peak at 952 cm^{-1} can be attributed to the Si–OH groups.[7] Furthermore, the peaks at 681 and 907 cm^{-1} were assigned to the Si–O symmetric stretching and to the Si–O in-plane stretching. The intermolecular interactions between the materials resulted in a shift in the bending vibrations of C–H at 1400 and 1705 cm^{-1} and the disappearance of the COO^- group peak at 1572 cm^{-1}. This may be due to the hydrogen bonding or dipole–dipole or electrostatic interactions between GC and SiO_2, which were improved by heat energy and high-speed stirring.[24−26] The FT-IR results demonstrate the presence of SiO_2 and octadecyldimethyl-(3-trimethoxysilylpropyl)-ammonium chloride (ODDMAC) and their bonding with GC in the composite films.

2.2. X-ray Diffraction (XRD) Analysis. Figure 2 presents the wide-angle XRD patterns of the GC and GC–SiO_2 nanocomposite films, which exhibited single broad amorphous

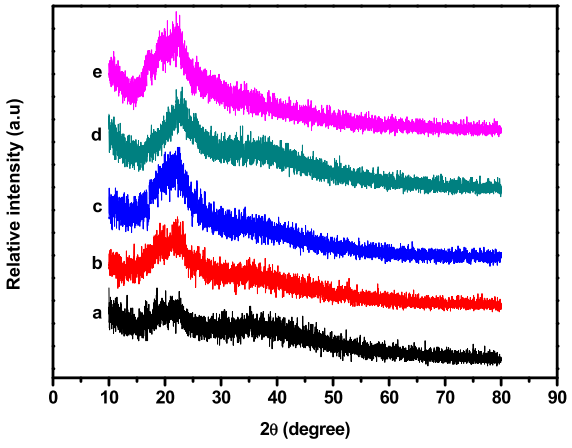

Figure 2. XRD patterns of (a) GC, (b) GC–SiO_2-1, (c) GC–SiO_2-3, (d) GC–SiO_2-5, and (e) GC–SiO_2-5 with ODDMAC.

https://dx.doi.org/10.1021/acsomega.0c04087
ACS Omega 2020, 5, 28767−28775

peaks at a 2θ value of approximately 22°. However, at high concentrations of SiO_2 (e.g., GC−SiO_2-5), the intensity of the peak increased. Overall, there were no significant changes in the structure of the films. This may be due to the uniform dispersion and distribution of SiO_2 in the polymer surface without changing the structure of the GC composites during the preparation process.

2.3. UV Spectral Analysis. The results of the UV−vis spectroscopies of the GC and GC−SiO_2 nanocomposites are shown in Figure 3 and Table 1. As shown in Figure 3, the GC

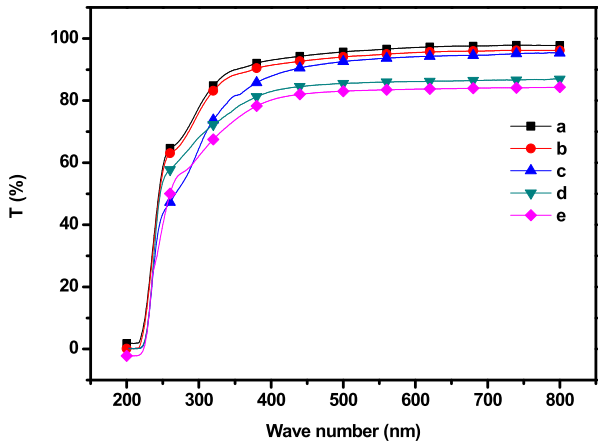

Figure 3. UV-transmittance spectra of (a) GC, (b) GC−SiO_2-1, (c) GC−SiO_2-3, (d) GC−SiO_2-5, and (e) GC−SiO_2-5 with ODDMAC.

and GC−SiO_2 composites containing 0−3 wt % of SiO_2 exhibited high optical transparency over the entire range of the visible region, likely because the SiO_2 particles were dispersed uniformly in the GC matrix without any aggregation. When the SiO_2 concentration was above 5 wt %, the optical transparency decreased gradually due to the separation of the interface between the GC and SiO_2 particles. Overall, the addition of nano-SiO_2 increased the UV light resistance of the nanocomposite films but decreased their transparency. For the highest loading of SiO_2 (5 wt %), the transmittance at 600 nm was 83.7% compared with 97.1% for pure GC. The transmittances of GC, GC−SiO_2, and GC−SiO_2 with ODDMAC at both 800 and 600 nm were in the ranges of 98.1−84.29% and 97.1−83.7%, respectively. All of the GC and GC−SiO_2 films are transparent with slight redness and yellowness (a^* and b^*, respectively, in Table 1). With the incorporation of SiO_2, the lightness (L^*) of the film decreased slightly, while a^* and b^* increased significantly. However, the color parameters remain unchanged to the naked eye.

2.4. Thermogravimetric Analysis (TGA). The effect of nano-SiO_2 on the thermal stability of the GC composites under nitrogen and oxygen atmospheres is shown in Figure 4 and Table 2. The temperatures at a gravimetric weight loss of 5% ($T_{5\%}$) and 10% ($T_{10\%}$) were taken as the specific temperatures of the degradation process. The neat GC composite film exhibited lower thermal stability than the GC−SiO_2-based films. The $T_{5\%}$ and $T_{10\%}$ values of the GC and GC−SiO_2 nanocomposite films were in the range of 99.4−128.6 °C and 131−169.2 °C, respectively. The addition of 1 wt % of SiO_2 improved $T_{5\%}$ by 10%, and 5 wt % of SiO_2 improved it by 29.3%. Similarly, the char yield of all of the prepared nanocomposite films was improved by the addition of SiO_2, where GC−SiO_2 exhibited the highest value (29.9%). The $T_{5\%}$ gravimetric weight loss of composite films is in the range of 61.9−113.4 °C, and the char yield is in the range of 13.4−26.6%. The thermal behavior was significantly reduced in an oxygen atmosphere, which is mainly due to the thermo-oxidative reaction induced by oxygen with an increase in the rate of decomposition. Moreover, the addition of ODDMAC to the GC−SiO_2 composites slightly improved the thermal stability. The derivative thermogravimetric (DTG) curves of the prepared nanocomposites are shown in Figures S1 and S2. It shows that the maximum degradation temperatures were between 180 and 320 °C for both under nitrogen and oxygen atmospheres. Moreover, it is also observed that the addition of Si nanoparticles shifted the DTG curves to slightly higher temperatures than those of neat GC composite films.

2.5. Scanning Electron Microscopy (SEM) Analysis. The surface morphology of the GC composite with various SiO_2 concentrations is shown in the SEM images (Figures 5 and S3). The neat GC exhibited a smooth and uniform surface morphology. The addition of SiO_2 to the GC matrix resulted in the SiO_2 particles being detected as small white dots. The films with lower silica contents were smoother, and the particles were evenly distributed on the surface. However, at a higher silica content (5 wt %), the number of large aggregates increased significantly. It can be seen that the morphology transforms from smooth to rough with increasing silica content. This result indicates that a large number of silica particles saturated the GC matrix. This supports the view that as the silica concentration increases, the size of the silica aggregates increases due to the strong interaction among the nanoparticles.[27] A similar result of silica nanocomposites was reported previously.[6,7,16] The energy dispersive X-ray (EDX) analysis of GC−SiO_2-5 reveals the presence of elements such as C, O, Na, and Cl along with Si in GC−SiO_2 composites. This data confirms the homogenous distribution of C, O, and Si in GC−SiO_2 composites and displays a well-defined compositional profile of the hybrid.

2.6. Mechanical Properties. The mechanical properties of the polymer composite films, particularly tensile strength (TS) and elongation at break (EB), are important for food packaging applications because they are the main indicators of the package integrity and its ability to withstand different environmental conditions. The TS and EB of the GC

Table 1. UV-Transmittance, Thickness, and Color Values of Gellan Gum, Sodium Carboxymethyl Cellulose, and SiO_2 Nanocomposite Films

sample	thickness (mm)	transmittance (%) at 600 nm	lightless (L^*)	redness (a^*)	yellowness (b^*)
GC	0.05	97.1	85.69	0.09	0.18
GC−SiO_2-1	0.06	95.5	84.40	0.14	0.25
GC−SiO_2-3	0.06	94.1	84.37	0.15	0.36
GC−SiO_2-5	0.07	86.1	84.31	0.21	0.60
GC−SiO_2-5 with ODDMAC	0.06	83.7	82.88	0.32	1.16

https://dx.doi.org/10.1021/acsomega.0c04087
ACS Omega 2020, 5, 28767−28775

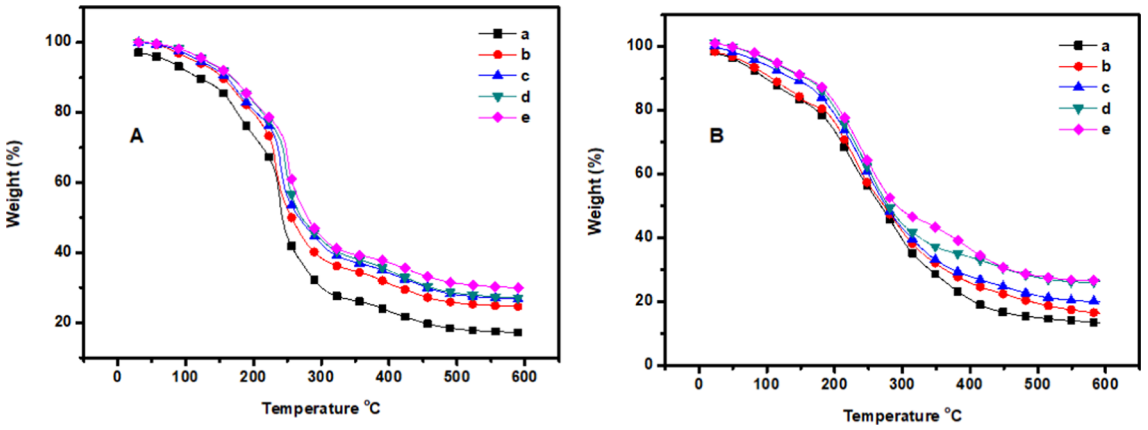

Figure 4. TGA analysis under a (A) N_2 atmosphere and an (B) O_2 atmosphere of (a) GC, (b) GC−SiO_2-1, (c) GC−SiO_2-3, (d) GC−SiO_2-5, and (e) GC−SiO_2-5 with ODDMAC.

Table 2. Thermal Properties of the GC and GC−SiO_2 Nanocomposite Films

	under a N_2 atmosphere			under an O_2 atmosphere		
sample	$T_{5\%}$	$T_{10\%}$	CY (%)	$T_{5\%}$	$T_{10\%}$	CY (%)
GC	99.4	146.4	20.1	61.9	98.7	13.4
GC−SiO_2-1	110.3	153.8	24.6	68.6	107.9	16.4
GC−SiO_2-3	117.7	160.5	26.1	91.2	138.3	20.1
GC−SiO_2-5	127.4	168.4	26.9	108.3	156.5	25.3
GC−SiO_2-5 with ODDMAC	128.6	169.2	29.9	113.4	160.5	26.2

composites increased as the content of SiO_2 increased (Table 3). This improvement is due to the strong interfacial adhesion and interaction between GC and the SiO_2 nanoparticles driven by van der Waals interactions and hydrogen bonding. The TS and EB of the GC−SiO_2 nanocomposite films are in the ranges of 28.2−49.6 and 23.1−37.4%, respectively. The TS likely increased due to the entanglement of the GC and SiO_2 components. The SiO_2 nanoparticles significantly improved the TS of the GC composite film, which may be attributed to the excellent compatibility of the components, the strong electrostatic interactions, and the resulting stable entanglements.

The EB of the GC composites improved from 23.1 to 37.4% with the addition of SiO_2. The SiO_2 nanoparticles plasticized, dispersed homogeneously, and aggregated slightly in the nanocomposite film. This result is in agreement with that reported in previous studies.[14] Overall, valuable and meaningful mechanical properties were obtained for GC−SiO_2 nanocomposite films.

2.7. Water Vapor Permeability (WVP). The WVP of biopolymer-based composite film packaging is an important parameter for maintaining the quality of food or pharmaceutical products. Polymer−inorganic hybrid materials can be used for packaging applications, in which the nanodispersed SiO_2 reduces the water barrier properties of polymer composites. The presence of SiO_2 in the polymer composites increases the diffusion distance by creating a tortuous path that the diffusing species must traverse.[28] The addition of SiO_2 nanoparticles in

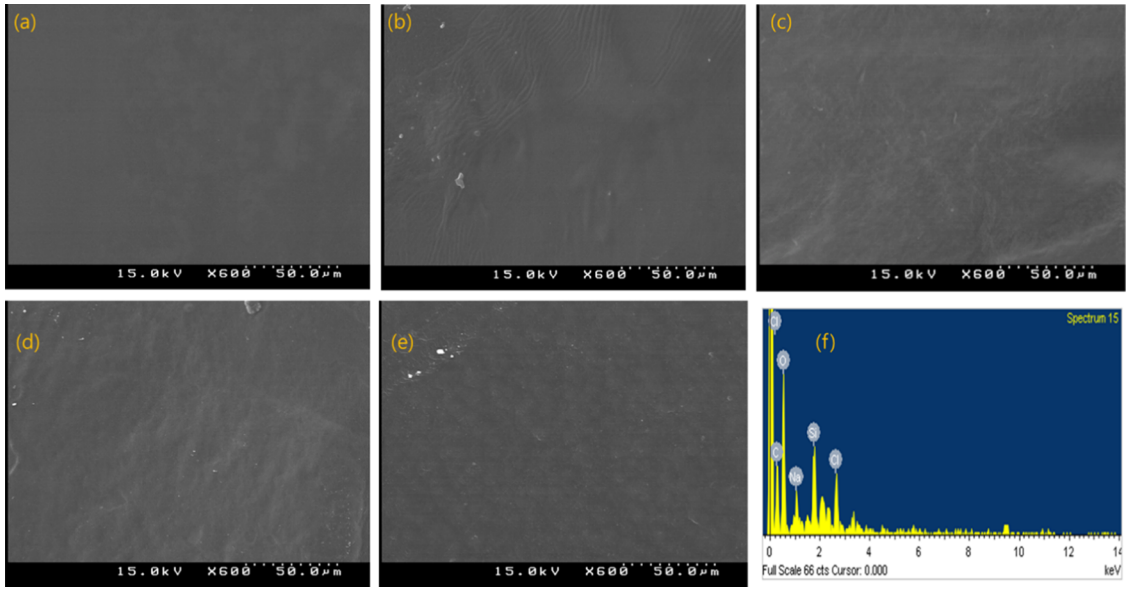

Figure 5. SEM images of (a) GC, (b) GC−SiO_2-1, (c) GC−SiO_2-3,(d) GC−SiO_2-5, and (e) GC−SiO_2-5 with ODDMAC; (f) EDX spectrum of GC−SiO_2-5.

https://dx.doi.org/10.1021/acsomega.0c04087
ACS Omega 2020, 5, 28767−28775

Table 3. Mechanical, Water Vapor Permeability, and Contact Angle Properties of the GC and GC−SiO_2 Nanocomposite Films

sample	tensile strength (MPa)	elongation at break (%)	water vapor permeability ($\times 10^{-9}$ g m/(m^2 Pa s))	water contact angle (°)
GC	28.2	23.1	4.1	52.4
GC−SiO_2-1	32.8	26.7	3.7	55.5
GC−SiO_2-3	38.0	29.4	3.1	57.3
GC−SiO_2-5	45.1	34.2	2.4	62.7
GC−SiO_2-5 with ODDMAC	49.6	37.4	1.9	67.5

the GC matrix reduced the WVP values from 4.1×10^{-9} to 2.4×10^{-9} g m/(m^2 Pa s) (Table 3). The WVP was further reduced to 1.9×10^{-9} g m/(m^2 Pa s) with the incorporation of ODDMAC. In general, water molecules easily diffuse through biopolymers in the presence of hydroxyl groups. Therefore, the primary reason for the reduction in the WVP was the formation of a denser polymer matrix structure in the GC−SiO_2−ODDMAC nanocomposite as compared with the neat or unfilled GC composite films.

2.8. Water Contact Angle (WCA). The results of the water contact angle (WCA) analysis of the prepared GC−SiO_2 composite films are shown in Table 3. The WCA of the neat GC composite was 52.4°, which was smaller than that of the GC−SiO_2 nanocomposites, which achieved a WCA of approximately 55.5−67.5° and exhibited hydrophobic properties. In addition, the WCA increased significantly with the addition of ODDMAC because the long alkyl chain containing silicone reacted with the hydroxy group of the GC−SiO_2 nanocomposite surface. In general, a rough surface has higher hydrophobicity than a flat surface. With the presence of silica nanoparticles, the rough surface and long alkyl chain groups caused the GC composite film to become significantly more hydrophobic.[29] The increased hydrophobicity of the prepared nanocomposites prevents the intrusion of water into the nanocomposites, resulting in an improvement in the contact angle.

2.9. Rheological Properties. Rheology is the study of the deformation and flow of materials. This characterization is useful in defining the interactions between the different components within a material. In this analysis, we studied the effect of different concentrations of SiO_2 nanoparticles on GC composites. The results indicated that the viscosities were dependent on the shear rate behaving like that of non-Newtonian fluids, suggesting the shear-thinning properties of the GC nanocomposites.[1,30,31] Figure 6 shows the viscosity of the GC−SiO_2 composites versus the shear rate. The shear viscosity of the GC composites increased as the concentration of SiO_2 increased. At a shear rate of 1.02, the shear viscosity of the neat GC composites was 115 Pa s, which increased to 250.2 for the GC−SiO_2 ODDMAC nanocomposites. This may be due to the strong interaction between GC and SiO_2 caused by the formation of H-bonds. However, at high shear rates, the shear degradation of the GC−SiO_2 nanocomposites was lower.

Moreover, there is a disruption of the molecular arrangement, resulting in a decrease in apparent viscosity. The relationship between the shear stress and shear rate of the GC−SiO_2 nanocomposite is shown in Figure 7. In the region of low shear rate, there was a significant increase in shear stress from 342.0 to 413.1 Pa at a shear rate of 1.02 s^{-1} for GC and GC−SiO_2-5 with ODDMAC nanocomposites. For shear rates beyond 40.0 s^{-1}, there was a negligible decrease in the shear stress of all composites. The incorporation of SiO_2 nanoparticles in the GC composites enhanced the shear stress, which was due to the interaction between the components.

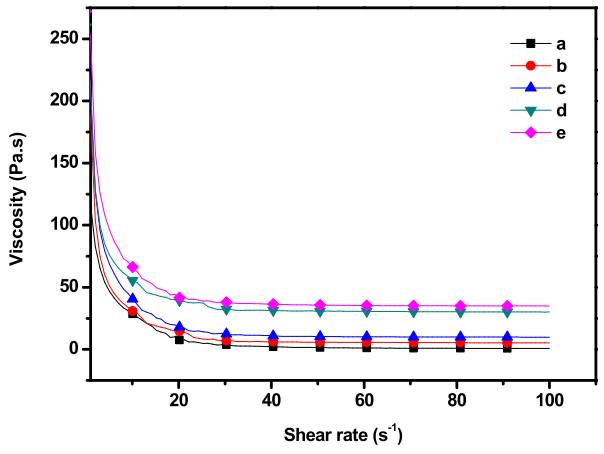

Figure 6. Shear viscosity of (a) GC, (b) GC−SiO_2-1, (c) GC−SiO_2-3,(d) GC−SiO_2-5, and (e) GC−SiO_2-5 with ODDMAC.

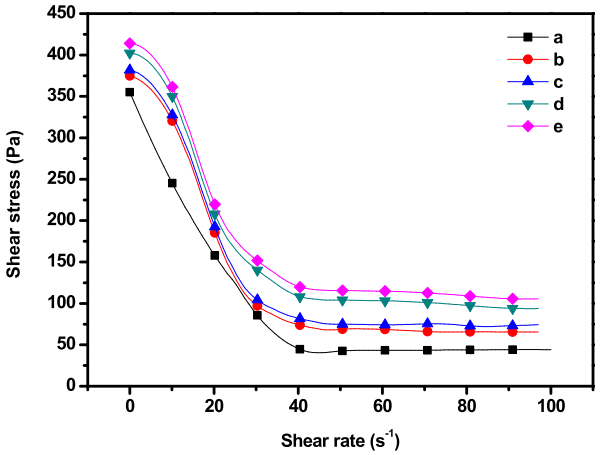

Figure 7. Flow curves of (a) GC, (b) GC−SiO_2-1, (c) GC−SiO_2-3, (d) GC−SiO_2-5, and (e) GC−SiO_2-5 with ODDMAC.

Dynamic shear measurement is related to the nature of the gel and its microstructure. The elastic (storage) modulus (G'), viscous (loss) modulus (G''), and complex viscosity of the GC composites were measured with different concentrations of SiO_2 nanoparticles (Figures 8 and 9−10) at a 0.1−100 Hz sweep frequency range. G′ represents the elastic energy temporarily stored in the gels to resist deformation, and G″ represents the stress energy used to initiate flow and transform energy into shear heat.[32] The behaviors of the hydrogel during dynamic shear measurement can be divided into strong and soft gels. Both G' and G'' increased as frequency increased, exhibiting shear-thinning behavior, while G' was higher in magnitude than G'' over the entire frequency range. The addition of SiO_2 nanoparticles significantly improved both G' and G''. G' exhibited a substantial elastic response, suggesting

https://dx.doi.org/10.1021/acsomega.0c04087
ACS Omega 2020, 5, 28767−28775

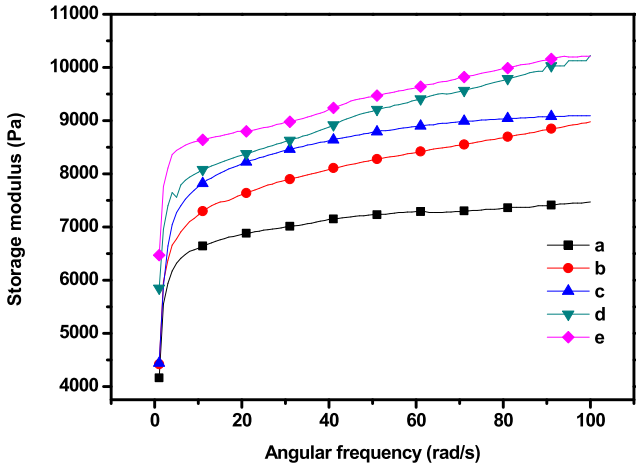

Figure 8. Storage modulus of (a) GC, (b) GC−SiO_2-1, (c) GC−SiO_2-3,(d) GC−SiO_2-5, and (e) GC−SiO_2-5 with ODDMAC.

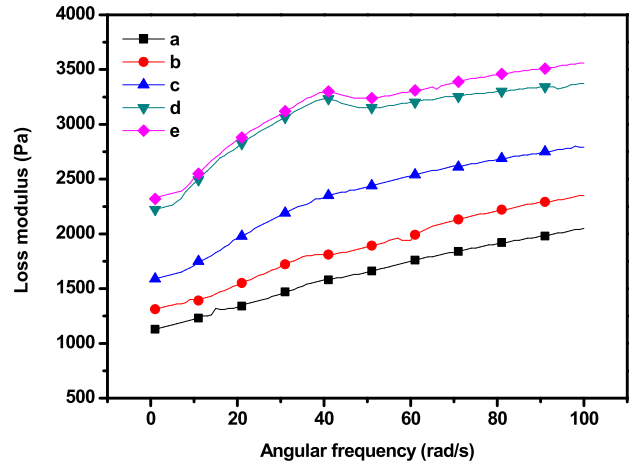

Figure 9. Loss modulus of (a) GC, (b) GC−SiO_2-1, (c) GC−SiO_2-3, (d) GC−SiO_2-5, and (e) GC−SiO_2-5 with ODDMAC.

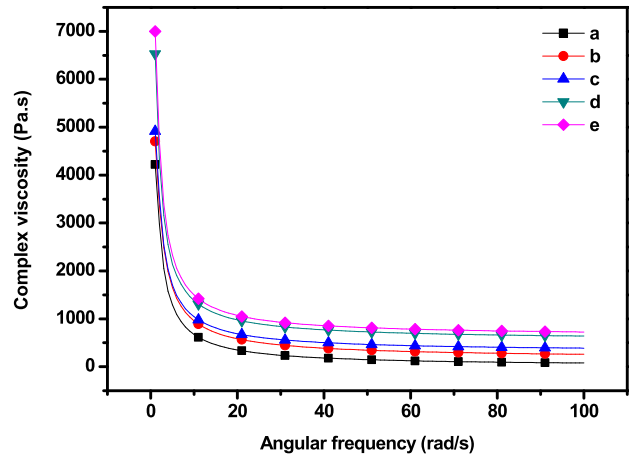

Figure 10. Complex viscosity of (a) GC, (b) GC−SiO_2-1, (c) GC−SiO_2-3,(d) GC−SiO_2-5, and (e) GC−SiO_2-5 with ODDMAC.

the solidlike and elastic properties of the cross-linked hydrogel. Both moduli increased rapidly at low frequencies, corresponding to the region of gel transition and gel growth, whereas they reached a plateau in the region corresponding to the post-cross-linking reaction.[33] In addition, the poor dependency of both moduli on frequency was due to the physical, non-permanent nature of the network at low frequencies. G' being larger than G'' is consistent with a matrix that behaves like an elastic solid. Neither the crossover point between the moduli nor any region shift was observed. In the frequency range tested, the matrix behaved like a stable viscoelastic solid, exhibited the behavior typical of a soft gel, and showed dispersion with a weak structure.

Furthermore, the complex viscosity versus frequency of the GC−SiO_2 composites is shown in Figure 10. The complex viscosity decreased significantly at low frequencies and was nonlinear. The addition of SiO_2 nanoparticles increased the complex viscosity of the GC composite hydrogel, which may induce a change in the interaction between the components, thereby changing the GC composite gel behavior.

2.10. Antimicrobial Properties. The antimicrobial activities of the GC, GC−SiO_2, and GC−SiO_2−ODDMAC nanocomposites were tested against 6 different bacterial pathogens (*Staphylococcus aureus*, *Bacillus cereus*, *Cronobacter sakazakii*, *Salmonella enterica*, *Salmonella typhimurium*, and *Escherichia coli*) and examined using the well-diffusion method. The test was conducted with different bacterial concentrations to 500 μg/well. The results indicate that the GC−SiO_2 with ODDMAC film exhibits a broad spectrum of antimicrobial activities at bacterial concentrations of 500 μg (Figure 11 and Table S1). It is effective for both Gram-positive and Gram-negative pathogens. Furthermore, the GC−SiO_2-5 ODDMAC nanocomposite was more active against *S. aureus* (inhibition zone of 34 mm) and less active against *B. cereus* (inhibition zone of 9 mm). The GC−SiO_2-5 with ODDMAC nanocomposites showed sufficient inhibition zones against Gram-negative pathogens, such as *C. sakazakii* (inhibition zone of 15 mm), *S. enterica* (inhibition zone of 15 mm), *S. typhimurium* (inhibition zone of 17 mm), and *E. coli* (inhibition zone of 18 mm). Quaternary ammonium silane prevents the adhesion of microorganisms on the surface owing to its hydrophobic properties and easily penetrates the cell membrane to inhibit microbial growth. A moderate to nil antimicrobial activity was observed in the GC and GC−SiO_2 samples. These results further support the studies of GC−SiO_2-5 with ODDMAC as an effective antimicrobial material.[21,22,34]

3. CONCLUSIONS

A novel homogeneous and reinforced GC nanocomposite film with SiO_2 nanoparticles was successfully prepared by the traditional solution casting method. The microstructure of the composite material was investigated by SEM analysis, revealing the uniform distribution of the SiO_2 nanoparticles on the surface. According to the structural analysis, the most probable mechanism of interaction between organic and inorganic components within the nanocomposite film is the formation of new hydrogen bonds. The rheological behavior of the GC composites was significantly influenced by the presence of the SiO_2 nanoparticles. The viscosity of the polymer decreased as the sweep frequency increased. At a given shear rate, the apparent viscosity decreased as the SiO_2 concentration increased.

This work also examined the rheological properties of GC−SiO_2 nanocomposites under different frequencies and shear rates. The addition of SiO_2 nanoparticles was found to significantly improve the rheological properties of GC composites, especially at high frequencies. The tensile strength and thermal stability of the GC−SiO_2 nanocomposite films

https://dx.doi.org/10.1021/acsomega.0c04087
ACS Omega 2020, 5, 28767−28775

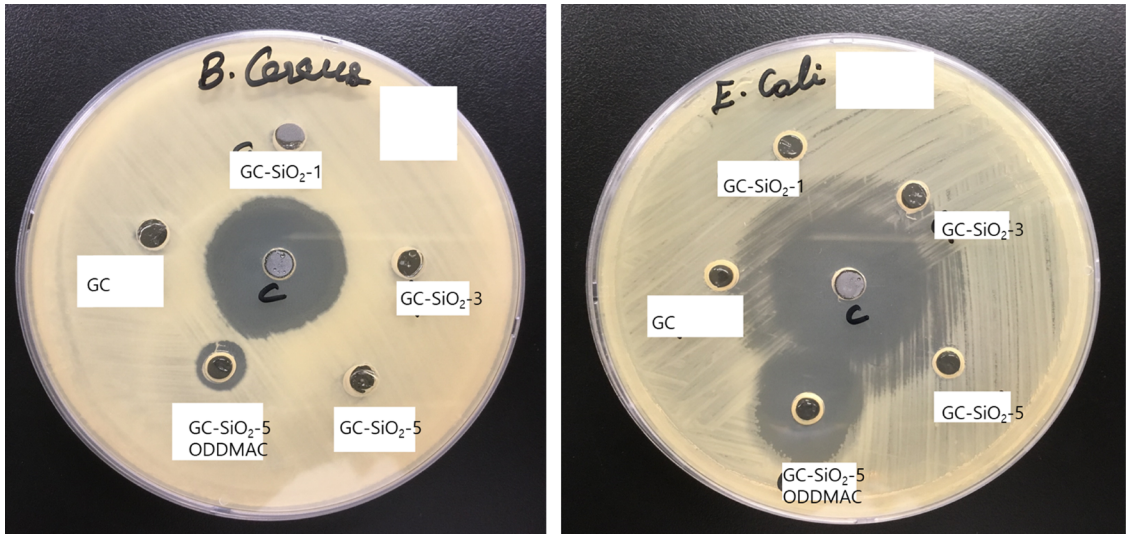

Figure 11. Representative image showing the antibacterial activity of positive control (*Streptomycin*) GC and GC−SiO_2-5 with ODDMAC against *B. cereus* and *E. coli*.

increased significantly. The GC−SiO_2 with ODDMAC film possessed the highest water contact angle and lowest WVP values, indicating that the addition of SiO_2 nanoparticles could enhance the hydrophobicity of the film. Similarly, nano-SiO_2 enhanced the UV light barrier properties of the films and slightly decreased their transparency.

Finally, the GC−SiO_2 films exhibited significant antimicrobial effects against Gram-positive and Gram-negative pathogens, and the GC−SiO_2-5 with ODDMAC nanocomposites dispersed well and showed effective antibacterial activities against six different pathogens. In summary, GC−SiO_2-5 nanocomposite films with robust mechanical and thermal properties and low WVP were produced by a simple, efficient, low-cost, and scalable method.

4. MATERIALS AND METHODS

4.1. Materials. Gellan gum (low acyl content) and polyacrylamide were purchased from TCI Chemicals, South Korea. SiO_2 (particle size <50 nm, Brunauer−Emmett−Teller (BET)) was purchased from Sigma Aldrich, South Korea. Glycerin, sodium citrate, sodium chloride, and citric acid were purchased from Dajang Chemicals, South Korea. Octadecyldimethyl-(3-trimethoxysilylpropyl)ammonium chloride (ODDMAC, 72% in ethanol, Biosafe SIO 6619.2) was obtained from KISCO, South Korea.

4.2. Production of GC−SiO_2 Nanocomposite Films. The GC−SiO_2 with ODDMAC nanocomposites were prepared by the solvent casting method using silica nanoparticles in different weight percentages (with 0, 1, 3, and 5 wt % SiO_2). Initially, gellan gum (1.0 g) and sodium carboxymethyl cellulose (1.0 g) were dispersed in glycerin (2 g) to avoid particle agglomeration during the process. The dispersion was mixed with distilled water (95 mL) and stirred for 30 min at 80 °C. Simultaneously, citric acid (0.5 g) and sodium citrate (1.0 g) were added under the same conditions. SiO_2 was dispersed separately in ethanol (15 mL) for 60 min at 50 °C. Dispersed SiO_2 was mixed with the reaction mixture and stirred under the same conditions. For the relevant samples, ODDMAC (0.25 g) was added to the reaction mixture and, after 30 min, the temperature was reduced to 55−60 °C with continuous stirring. Finally, the obtained GC−SiO_2 with ODDMAC nanocomposite solution was spread uniformly onto a glass surface, and after one week, it was peeled off from the glass plate under dry conditions. Similarly, all other composite films, namely, neat GC (no SiO_2), GC−SiO_2-1 (1 wt % of SiO_2), GC−SiO_2-3 (3 wt % of SiO_2), GC−SiO_2-5 (5 wt % of SiO_2), and GC−SiO_2-5 with ODDMAC (5 wt % of SiO_2 and 0.2 g of ODDMAC), were prepared and studied.

■ ASSOCIATED CONTENT

Supporting Information

The Supporting Information is available free of charge at https://pubs.acs.org/doi/10.1021/acsomega.0c04087.

Characterization methods, DTG curves, table of microbial properties, SEM-EDX images (PDF)

■ AUTHOR INFORMATION

Corresponding Author

Jaewoong Lee − *Department of Fiber System Engineering, Yeungnam University, Gyeongsan-si, Gyeongsangbuk-do 38541, South Korea*; Phone: +82-53-810-2786; Email: jaewlee@yu.ac.kr; Fax: +82-53.810.4685

Authors

Balasubramanian Rukmanikrishnan − *Department of Fiber System Engineering, Yeungnam University, Gyeongsan-si, Gyeongsangbuk-do 38541, South Korea*; orcid.org/0000-0001-6207-7271

Chaehyun Jo − *Department of Fiber System Engineering, Yeungnam University, Gyeongsan-si, Gyeongsangbuk-do 38541, South Korea*

Seungjin Choi − *Department of Fiber System Engineering, Yeungnam University, Gyeongsan-si, Gyeongsangbuk-do 38541, South Korea*

Srinivasan Ramalingam − *Department of Food Science and Technology, Yeungnam University, Gyeongsan-si, Gyeongsangbuk-do 38541, South Korea*

Complete contact information is available at: https://pubs.acs.org/10.1021/acsomega.0c04087

https://dx.doi.org/10.1021/acsomega.0c04087
ACS Omega 2020, 5, 28767−28775

Notes

The authors declare no competing financial interest.

■ ACKNOWLEDGMENTS

This work was supported by the Korea Institute for Advancement of Technology (KIAT) grant (P0012770) funded by the South Korean government (Ministry of Trade, Industry, and Energy-MOTIE).

■ REFERENCES

(1) Wang, B.; Xiaodeng, Y.; Congde, Q.; Yan, L.; Tianduo, L.; Chunlin, X. Effects of chitosan quaternary ammonium salt on the physicochemical properties of sodium carboxymethyl cellulose-based films. *Carbohydr. Polym.* **2018**, *184*, 37−46.

(2) Suo, A.; Junmin, Q.; Yu, Y.; Wanggang, Z. Synthesis and Properties of Carboxymethyl Cellulosegraft-Poly(acrylic acid-co-acrylamide) as a Novel Cellulose-Based Superabsorbent. *J. Appl. Polym. Sci.* **2007**, *103*, 1382−1388.

(3) Aravind, N.; Mike, S.; Christopher, M. F. Effect of soluble fibre (guar gum and carboxymethylcellulose) addition on technological, sensory and structural properties of durum wheat spaghetti. *Food Chem.* **2012**, *131*, 893−900.

(4) Byras, J. A.; George, F. F.; James, A. K.; Frederick, C. F. Influence of pH and temperature on the rheological properties of aqueous dispersions of starch−sodium palmitate complexes. *Carbohydr. Polym.* **2012**, *88*, 91−95.

(5) Wang, Y.; Chen, D. Preparation and characterization of a novel stimuli-responsive nanocomposite hydrogel with improved mechanical properties. *J. Colloid Interface Sci.* **2012**, *372*, 245−251.

(6) Song, H.; Liwei, Z. Nanocomposite films based on cellulose reinforced with nano-SiO2: microstructure, hydrophilicity, thermal stability, and mechanical properties. *Cellulose* **2013**, *20*, 1737−1746.

(7) Rangelova, N.; Lyubomir, A.; Tsvetelina, A.; et al. Preparation and characterization of SiO2/CMC/Ag hybrids with antibacterial properties. *Carbohydr. Polym.* **2014**, *101*, 1166−1175.

(8) Zhang, L. M.; Tao, K. Aqueous polysaccharide blends based on hydroxypropyl guar gum and carboxymethyl cellulose: synergistic viscosity and thixotropic properties. *Colloid Polym. Sci.* **2006**, *285*, 145−151.

(9) Yang, S.; Yanjun, T.; Junming, W.; Fangong, K.; Junhua, Z. Surface Treatment of Cellulosic Paper with Starch-Based Composites Reinforced with Nanocrystalline Cellulose. *Ind. Eng. Chem. Res.* **2014**, *53*, 13980−13988.

(10) Ten, E.; David, F. B.; Bin, L.; Long, J.; Michael, P. W. Effects of Cellulose Nanowhiskers on Mechanical, Dielectric, and Rheological Properties of Poly(3-hydroxybutyrate-co-3-hydroxyvalerate)/Cellulose Nano whisker Composites. *Ind. Eng. Chem. Res.* **2012**, *51*, 2941−2951.

(11) Shin, H.; Bradley, D. O.; Ali, K. The mechanical properties and cytotoxicity of cell-laden double-network hydrogels based on photocrosslinkable gelatin and gellan gum biomacromolecules. *Biomaterials* **2012**, *33*, 3143−3152.

(12) Tang, Y.; Jing, S.; Hongsong, F.; Xingdong, Z. An improved complex gel of modified gellan gum and carboxymethyl chitosan for chondrocytes encapsulation. *Carbohydr. Polym.* **2012**, *88*, 46−53.

(13) García-Abuín, A.; Diego, G. D.; José, M. N.; Lourdes, C. Q. R. Viscosimetric behaviour of carboxymethyl cellulose − Arabic gum mixtures: A new step to modelling. *Carbohydr. Polym.* **2010**, *80*, 26−30.

(14) Hou, X.; Zhixin, X.; Yanzhi, X.; Yimin, Q.; Guofang, Z.; Hongwu, L.; Kechang, L. Effect of SiO2 nanoparticle on the physical and chemical properties of eco-friendly agar/sodium alginate nanocomposite film. *Int. J. Biol. Macromol.* **2019**, *125*, 1289−1298.

(15) Huang, Q.; Manman, X.; Runcang, S.; Xiaohui, W. Large scale preparation of graphene oxide/cellulose paper with improved mechanical performance and gas barrier properties by conventional papermaking method. *Ind. Crops Prod.* **2016**, *85*, 198−203.

(16) Angelova, T.; Nadezhda, R.; Ruslan, Y. Nelly Georgieva, Rudolf Müller, Antibacterial activity of SiO2/hydroxypropyl cellulose hybrid materials containing silver nanoparticles. *Mater. Sci. Eng., C* **2012**, *32*, 1241−1246.

(17) Shoichiro, Y.; Hideaki, M.; Megumi, N.; Toshiki, H.; Takashi, S. Preparation and mechanical properties of bacterial cellulose nanocomposites loaded with silica nanoparticles. *Cellulose* **2008**, *15*, 111−120.

(18) Romero-Bastida, C. A.; Miguel, C. G.; Luis, A. B. P.; Estefania, A. R.; Gonzalo, V.; Guadalupe, M. M. Rheological properties of nanocomposite-forming solutions and film based on montmorillonite and corn starch with different amylose content. *Carbohydr. Polym.* **2018**, *188*, 121−127.

(19) Sriya, D.; Fahmida, I.; Lan, M.; Sanjoy, K. B.; Ronald, C. H.; Micah, J. G. Rheology and Morphology of Pristine Graphene/Polyacrylamide Gels. *ACS Appl. Mater. Interfaces* **2013**, *5*, 8633−8640.

(20) Yang, J.; Deng, L. H.; Han, C. R.; Duan, J. F.; Ma, M. G.; Zhang, X. M.; Feng, X.; Sun, R. C. Synthetic and viscoelastic behaviors of silica nanoparticle reinforced poly(acrylamide) core−shell nanocomposite hydrogels. *Soft Matter* **2013**, *9*, 1220−1230.

(21) Liu, Y.; Kaikai, M.; Xuehong, R.; Huang, T. S.; et al. Antibacterial cotton treated with N-halamine and quaternary ammonium salt. *Cellulose* **2013**, *20*, 3123−3130.

(22) Li, H.; Hongqian, B.; Ke, X. B.; Lee, C. Y.; Bo, L.; Zin, M. T.; Lifeng, K. High durability and low toxicity antimicrobial coatings fabricated by quaternary ammonium silane copolymers. *Biomater. Sci.* **2016**, *4*, 299−309.

(23) Elena, P.; Klein, M. Formation of contact active antimicrobial surfaces by covalent grafting of quaternary ammonium compounds. *Colloids Surf., B* **2018**, *169*, 195−205.

(24) Tang, H.; Hanguo, X.; Shangwen, T.; Peng, Z. A Starch-Based Biodegradable Film Modified by Nano Silicon Dioxide. *J. Appl. Polym. Sci.* **2009**, *113*, 34−40.

(25) Parveen, A. S.; Thirukumaran, P.; Sarojadevi, M. Fabrication of highly durable hydrophobic PBZ/SiO2 surfaces. *RSC Adv.* **2015**, *5*, 43601−43610.

(26) Vijayakumar, V.; Dipak, K. Hybrid composite membranes of chitosan/sulfonated polyaniline/silica as polymer electrolyte membrane for fuel cells. *Carbohydr. Polym.* **2018**, *179*, 152−163.

(27) Li, Y.; Changyu, H.; Junjia, B.; Lijing, H.; Lisong, D.; Ge, G. Rheology and Biodegradation of Polylactide/Silica Nanocomposites. *Polym. Compos.* **2012**, *33*, 1719−1727.

(28) Chang, K. C.; Lin, C. Y.; Lin, H. F.; Chiou, S. C.; Huang, W. C.; Yeh, J. M.; Yang, J. C. Thermally and Mechanically Enhanced Epoxy Resin-Silica Hybrid Materials Containing Primary Amine-Modified Silica Nanoparticles. *J. Appl. Polym. Sci.* **2008**, *108*, 1629−1635.

(29) Liu, F.; Shuliang, W.; Ming, Z.; Miaolian, M.; Chengyu, W.; Jian, Li. Improvement of mechanical robustness of the superhydrophobic wood surface by coating PVA/SiO2 composite polymer. *Appl. Surf. Sci.* **2013**, *280*, 686−692.

(30) Li, X. Y.; Dong, L.; Wang, L. J.; Min, W.; Benu, A. The effect of addition of flaxseed gum on the rheological behavior of mixed flaxseed gum−casein gels. *Carbohydr. Polym.* **2012**, *88*, 1214−1220.

(31) Zheng, J.; Ruiqi, Z.; Fusheng, Z.; Jianquan, K. Effects of sodium carboxymethyl cellulose on rheological properties and gelation behaviors of sodium alginate induced by calcium ions. *LWT* **2019**, *103*, 131−138.

(32) Pahimanolis, N.; Arto, S.; Paavo, A. P.; Juuso, T. K.; Johansson, L. S.; Janne, R.; Ritva, S.; Jukka, S. Nanofibrillated cellulose/carboxymethyl cellulose composite with improved wet strength. *Cellulose* **2013**, *20*, 1459−1468.

(33) Gupta, A.; William, S.; Gregory, T. S.; Donald, H.; Eric, A. M. Rheological and Thermo-Mechanical Properties of Poly(lactic acid)/Lignin-Coated Cellulose Nanocrystal Composites. *ACS Sustainable Chem. Eng.* **2017**, *5*, 1711−1720.

(34) Michailidis, M.; Ioritz, S. B.; Evanthia, A. A.; Yuri, A. D. Fe.; Jenny, A.; Reut, W.; Dmitry, G.; Rasmita, R.; Yehuda, B.; Raechelle, A. D.; Dmitry, S. Modified Mesoporous Silica Nanoparticles with a Dual

https://dx.doi.org/10.1021/acsomega.0c04087
ACS Omega 2020, 5, 28767−28775

Synergetic Antibacterial Effect. *ACS Appl. Mater. Interfaces* **2017**, *9*, 38364−38372.

https://dx.doi.org/10.1021/acsomega.0c04087
ACS Omega 2020, 5, 28767−28775